CHARACTERIZATION OF NULL GEODESICS ON KERR SPACETIMES

CLAUDIO F. PAGANINI[†], BLAZEJ RUBA[‡] AND MARIUS A. OANCEA[*]

[†] *Albert Einstein Institute, Am Mühlenberg 1, D-14476 Potsdam, Germany*

[‡] *Faculty of Physics, Astronomy and Computer Science, Jagiellonian University, Lojasiewicza 11, 30-348 Cracow, Poland*

[*] *Faculty of Physics, Babes-Bolyai University, 400084, Cluj-Napoca, Romania*

Abstract. We consider null geodesics in the exterior region of a sub-extremal Kerr spacetime. We show that most well known fundamental properties of null geodesics can be represented in one plot. In particular, one can see immediately that the ergoregion and trapping are separated in phase space.
Furthermore, we show that from the point of view of any timelike observer outside of a black hole, trapping can be understood as a smooth sets of spacelike directions on the celestial sphere of the observer.

Contents

E-mail address: claudio.paganini@aei.mpg.de, blazej.ruba@student.uj.edu.pl, marius.oancea@aei.mpg.de.

Date: October 19, 2017 *File:Kerrnullgeod.tex*.

1. Introduction

In recent years there has been a lot of progress in the Kerr uniqueness and the Kerr stability problem. Having a thorough understanding of geodesic motion and in particular the behavior of null geodesics in Kerr spacetimes is helpful to understand many of the harder problems related to these spacetimes. In this paper we study the properties of null geodesics in the exterior region in the sub-extremal case, where $a \in [0, M)$. The geodesic structure of Kerr spacetimes has been subject of a lot of research. Our aim here is to give a unified and accessible presentation of the most important properties of geodesics in the Kerr spacetime, with regard to the open problems mentioned above. The Mathematica notebook that has been developed for this paper is intended to help the reader gain an intuition on the influence of various parameters on the geodesic motion, despite of the complexity of the underlying equations. It can be downloaded under the permanent link [1]. In Section 6 we explain where these plots give useful insights.

An extensive discussion of geodesics in Kerr spacetimes and many further references can for example be found in [4, p.318] and [15]. See [19] for a nice treatment of the trapped set in Kerr including many explicit plots of trapped null geodesics at different radii. Here we focus more on global properties of the null geodesics and less on the details of motion. Analyzing the turning points for a dynamical system is a powerful tool to extract information about its global behaviours. For example, in any $1+1$ dimensional system stable bounded orbits only exist if there exist two disjoint turning points in the spacial direction between which the system can oscillate. For geodesics in Kerr this has been studied in detail by Wilkins [20]. The techniques used here are very close to that paper. Many of the results discussed in the first four sections of this note are in fact well known, however our focus is on proving that all these properties can be read of from one simple plot. Thereby making it easier for people to understand the general behaviour of null geodesics in Kerr. Hence we do show that the various plots provided in the notebook actually do cover the whole space of relevant parameters. A different representation of the forbidden regions in phase space can be found in [15, p.214] and also in [17]. The presentation chosen here is adapted to help understand the phase space decomposition used in the proof for the decay of the scalar wave in subextremal Kerr [7].

The novel material in this note which is presented in the section 5 is related to the notion of black hole shadows. The shadow of the black hole is defined as the innermost trajectory on which light from a background source passing a black hole can reach the observer. The first discussion of the shadow in Schwarzschild spacetimes can be found in [18], and for extremal Kerr at infinity it was later calculated in [2]. Analyzing the shadows of black holes is of direct physical interest as there is hope for the Event Horizon Telescope to be able to resolve the black hole in the center of the Milky Way well enough that one can compare it to the predictions from theoretical calculations, see for example [8]. This perspective has led to a number of advancements in the theoretical treatment of black hole shadows in recent years [6, 9, 10, 11, 13, 14].

The novel material in the present work is the first rigorous proof of Theorem 14. The significance of Theorem 14 is due to the fact that for any subextremal Kerr spacetime, including Schwarzschild, the past and the future trapped sets at any point are topologically an S_1 on the celestial sphere of any observer in the exterior region. We would like to stress that Theorem 14 therefore describes a property of trapping which does not change when going from Schwarzschild to Kerr.

Further we present numerical evidence that the radial degeneracy for the shape of the shadow, as it exists in Schwarzschild and for observers on the symmetry axis of Kerr spacetimes, is broken away from the symmetry axis. For future observations

this means that the distance from the observed black hole can not be ignored when one tries to extract the black holes parameters from the shadow.

Overview of this paper. In section 2 we collect some background on the Kerr spacetime. We discuss its symmetries and the conserved quantities for null geodesic which arise from them in section 2.1. In section 3 we discuss the geodesic equations in its separated form, focusing on the radial and the θ equation. For the radial equation we show that many properties of its solutions can be understood from one plot. In section 4 we use the analysis of section 3 to discuss the properties of a number of special solutions. In particular we discuss the radially in-/outgoing null geodesics (i.e. the principal null directions) and the trapped set which are of relevance in the black hole stability problem. Next we discuss the **T**-orthogonal null geodesics which are relevant in the black hole uniqueness problem. We want to stress that most material in the sections up to this point is well known. The purpose here is to collect these facts and show that these properties can actually be understood from a few plots. In section 5 we prove a Theorem on the topological structure of the past and future trapped sets. In the same section we also present numerical evidence for a breaking of the radial degeneracy of the black hole shadows in Kerr spacetimes. Finally in section 6 we discuss how the plots developed for this paper can be used.

2. The Kerr Spacetime

The Kerr family of spacetimes describes axially symmetric, stationary and asymptotically flat black hole solutions to the vacuum Einstein field equations. We use Boyer-Lindquist (BL) coordinates (t, r, ϕ, θ), which have the property that the metric components are independent of ϕ and t. The metric has the form:

$$g = -\left(1 - \frac{2Mr}{\Sigma}\right)\mathrm{d}t^2 - \frac{2Mar\sin^2\theta}{\Sigma}2\mathrm{d}t\mathrm{d}\phi + \frac{\Sigma}{\Delta}\mathrm{d}r^2 + \Sigma\mathrm{d}\theta^2 + \frac{\sin^2\theta}{\Sigma}\mathcal{A}\mathrm{d}\phi^2, \quad (2.1)$$

where

$$\Sigma = r^2 + a^2\cos^2\theta, \quad (2.2)$$

$$\Delta(r) = r^2 - 2Mr + a^2 = (r - r_+)(r - r_-), \quad (2.3)$$

$$\mathcal{A} = (r^2 + a^2)^2 - a^2\Delta\sin^2\theta. \quad (2.4)$$

The zeros of $\Delta(r)$ are given by:

$$r_\pm = M \pm \sqrt{M^2 - a^2}, \quad (2.5)$$

and correspond to the location of the event horizon at $r = r_+$ and of the Cauchy horizon at $r = r_-$. In the present work we are only interested in the exterior region hence $r \in (r_+, \infty)$. For our considerations it is useful to introduce an orthonormal tetrad. A convenient choice is:

$$e_0 = \frac{1}{\sqrt{\Sigma\Delta}}\left((r^2 + a^2)\partial_t + a\partial_\phi\right), \quad (2.6a)$$

$$e_1 = \sqrt{\frac{\Delta}{\Sigma}}\partial_r, \quad (2.6b)$$

$$e_2 = \frac{1}{\sqrt{\Sigma}}\partial_\theta, \quad (2.6c)$$

$$e_3 = \frac{1}{\sqrt{\Sigma}\sin\theta}\left(\partial_\phi + a\sin^2\theta\partial_t\right). \quad (2.6d)$$

This frame is a natural choice as the principal null directions can be written in the simple form $e_0 \pm e_1$. These generate a congruences of radially outgoing and ingoing null geodesics. We will come back to this fact in section 4.1. For the further

considerations we will use e_0 as the local time direction. Furthermore we define the local rotation frequency of the black hole to be:

$$\omega(r) = \frac{a}{r^2 + a^2}, \tag{2.7}$$

which has the rotation frequency of the horizon as a limit for $r \searrow r_+$:

$$\omega_H = \omega(r_+). \tag{2.8}$$

The name choice for $\omega(r)$ is motivated by noting that a particle at rest in the local inertial frame given by the tetrad (2.6) will move in the ϕ direction in Boyer-Lindquist coordinates with $\frac{d\phi}{dt} = \omega(r)$ with respect to an observer at rest in this frame at infinity.

2.1. **Symmetries and Constants of Motion.** The independence of the metric components of the coordinates t and ϕ is a manifestation of the presence of two Killing vector fields $(\partial_t)^\nu$, $(\partial_\phi)^\nu$, which both satisfy the Killing equation:

$$\nabla_{(\mu} K_{\nu)} = 0 \tag{2.9}$$

and they commute. Furthermore the Kerr spacetime features an irreducible Killing tensor $\sigma_{\mu\nu}$, cf. [4, p.320]. It is symmetric and satisfies the Killing tensor equation:

$$\nabla_{(\alpha}\sigma_{\beta\gamma)} = 0 \tag{2.10}$$

but it can not be written as a linear combination of tensor products of Killing vectors. In terms of the tetrad (2.6) the Killing tensor can be written as:

$$\sigma_{\mu\nu} = -a^2 \cos^2\theta g_{\mu\nu} + \Sigma\left((e_2)_\mu (e_2)_\nu + (e_3)_\mu (e_3)_\nu\right). \tag{2.11}$$

In the limiting case $a = 0$ it takes the form:

$$\sigma^{(a=0)} = r^4(\mathrm{d}\theta^2 + \sin^2\mathrm{d}\phi^2). \tag{2.12}$$

This is the tensor field obtained by taking the sum of the second tensor product of the three generators of spherical symmetry. From the geodesic equation:

$$\dot\gamma^\mu \nabla_\mu \dot\gamma^\nu = 0 \tag{2.13}$$

and the Killing equations it follows that a contraction of the tangent vector $\dot\gamma^\mu$ of an affinely parametrized geodesic γ with a Killing tensor gives a constant of motion. In Kerr spacetimes those are the mass[1], the energy, the angular momentum with respect to the rotation axis of the black hole and Carter's constant [3]:

$$-m^2 = g_{\mu\nu}\dot\gamma^\mu\dot\gamma^\nu, \tag{2.14a}$$

$$E = -(\partial_t)^\nu \dot\gamma_\nu, \tag{2.14b}$$

$$L_z = (\partial_\phi)^\nu \dot\gamma_\nu, \tag{2.14c}$$

$$K = \sigma_{\mu\nu}\dot\gamma^\mu\dot\gamma^\nu. \tag{2.14d}$$

It follows from equation (2.12) that in a Schwarzschild spacetime K is the square of the total angular momentum of the particle. Carter's constant is non-negative for all time like or null geodesics, which can be seen immediately from equation (2.11) and the fact that $g_{\mu\nu}\dot\gamma^\mu\dot\gamma^\nu \leq 0$ for any future directed causal geodesic. In the case of $a \neq 0$ it is even strictly positive for any time like geodesic. It turns out that some combinations of these conserved quantities are more convenient to work with, so we give them their own names:

$$Q = K - (aE - L_z)^2, \tag{2.15}$$

$$L^2 = L_z^2 + Q. \tag{2.16}$$

One can think of L^2 as the total angular momentum of the particle, in the sense that it is this quantity that is replaced with the spheroidal eigenvalue in the potential

[1]The metric satisfies the Killing tensor equation (2.10) trivially and therefore it gives us a conserved quantity as well.

of the wave-equation, as we will show in Section 6. One can then think of Q as the component of the angular momentum in direction perpendicular to the rotation axis of the black hole.[2] It is important though that these interpretations should not be taken to strictly, because geodesics in Kerr spacetimes do not feature a conserved total angular momentum vector.

Remark 1. *In contrast to K, Q is not positive anymore but from the equation of motion that we will later define in* (3.1d) *we get the condition that $\Theta \geq 0$ for any geodesic to exist at a point and hence that:*

$$Q \geq -a^2 E^2 \cos^2 \theta \tag{2.17}$$

holds.

In the case of null-geodesics we can rescale the tangent vector without changing the properties of the geodesic. We will use this to reduce the number of parameters. We define the conserved quotients to be:

$$\mathcal{Q} = \frac{Q}{L_z^2}, \qquad \mathcal{E} = \frac{E}{L_z}. \tag{2.18}$$

An alternative set of conserved quotients is given by:

$$\mathcal{K} = \frac{K}{E^2}, \qquad \mathcal{L} = \frac{L_z}{E}. \tag{2.19}$$

These are more commonly used in the literature as they are more suited for certain calculations. However for the present work we will mostly use the first set.

Properties of the Killing Fields and Tensor. The vector field $(\partial_\phi)^\nu$ is spacelike for all $r > 0$. The vector field $(\partial_t)^\nu$ is timelike in the asymptotically flat region. It becomes spacelike in the interior of the *ergoregion*, which is defined by the inequality $g(\partial_t, \partial_t) \geq 0$ or in terms of BL-coordinates by $-\Delta + a^2 \sin^2 \theta \leq 0$. The case of equality determines the boundary of the ergoregion which is often referred to as the ergosphere. Solving for the case of equality we get the radius of the ergosphere to be:

$$r_{ergo}(\theta) = M + \sqrt{M^2 - a^2 \cos^2(\theta)}. \tag{2.20}$$

At the equator the ergosphere lies at $r = 2M$ while it corresponds to the horizon $r = r_+$ on the rotation axis.

As mentioned above the two Killing vector fields generate one-parameter groups of isometries. It is natural to ask if the Killing tensor present in the Kerr spacetimes can also be related to some sort of symmetry. This question can be answered using Hamiltonian formalism. For a Hamiltonian flow parametrized by λ with Hamiltonian H the derivative of any function $f(x, p)$ is given by the Poisson bracket:

$$\frac{\mathrm{d}f}{\mathrm{d}\lambda} = \{H, f\} \equiv \frac{\partial H}{\partial p_\mu}\frac{\partial f}{\partial x^\mu} - \frac{\partial H}{\partial x^\mu}\frac{\partial f}{\partial p_\mu}. \tag{2.21}$$

Each smooth function on phase space can be taken as a Hamiltonian and therefore gives rise to a local flow. Geodesic motion is generated by the function $-m^2$. E and L_z generate translations in t and ϕ. In the case $a = 0$ the function K generates rotations in the plane orthogonal to the particle's total angular momentum vector with angular velocity equal to the angular momentum of the particle. For rotating black holes it involves a change of all spatial coordinates, but it leaves quantities conserved under geodesic flow invariant. This flow explicitly depends on fiber coordinates p_μ and can not be projected to a symmetry of the spacetime manifold itself.

[2]The three quantities K, Q and L^2 are often labeled differently by different authors.

3. Geodesic Equations

We now focus our attention on null geodesics. The constants of motion introduced in (2.14) can be used to decouple the geodesic equation to a set of four first order ODEs, cf. [4, p. 242]:

$$\Sigma\Delta\dot{t} = \mathcal{A}E - 2MarL_z, \tag{3.1a}$$

$$\Sigma\Delta\dot{\phi} = 2MarE + (\Sigma - 2Mr)\frac{L_z}{\sin^2\theta}, \tag{3.1b}$$

$$\Sigma^2\dot{r}^2 = R(r, E, L_z, K) = ((r^2 + a^2)E - aL_z)^2 - \Delta K, \tag{3.1c}$$

$$\Sigma^2\dot{\theta}^2 = \Theta(\theta, E, L_z, Q) = Q - \left(\frac{L_z^2}{\sin^2\theta} - E^2a^2\right)\cos^2\theta, \tag{3.1d}$$

where the dot denotes differentiation with respect to the affine parameter λ. [3] For $L_z \neq 0$ the four equations are homogeneous in L_z, when written in terms of the conserved quotients. For the radial and the angular equations we have:

$$R(r, E, L_z, Q) = L_z^2 R(r, \mathcal{E}, 1, \mathcal{Q}), \tag{3.2}$$

$$\Theta(\theta, E, L_z, Q) = L_z^2\Theta(r, \mathcal{E}, 1, \mathcal{Q}). \tag{3.3}$$

Remark 2. *To avoid introducing new functions whenever we change between different sets of conserved quantities we use* $R(r, E, L_z, Q) = R(r, E, L_z, K(Q, L_z, E))$.

From the homogeneity of the equations of motion (3.1) we get that the only conserved quantities which affect the dynamics are conserved quotients like $\mathcal{E}$, $\mathcal{Q}$ or $\frac{\mathcal{Q}}{E^2}$ in the case of $L_z = 0$. This is due to the fact that an affine reparametrization $\lambda \mapsto \alpha\lambda$, $\dot{\gamma} \mapsto \alpha^{-1}\dot{\gamma}$ changes the values of E, L_z and Q while leaving the trajectories and the aforementioned quotients unchanged. The case $L_z = 0$ can be seen as the limit of $\mathcal{Q}$ and $\mathcal{E}$ tending to infinity. In these notes we will omit a separate discussion of this case as it is essentially equivalent to the Schwarzschild case and it is not needed for the understanding of the phase space decomposition in [7]. It is sufficient to consider future directed geodesics as the past directed case follows from the symmetry of the metric when replacing (t, ϕ) with $(-t, -\phi)$.
In Schwarzschild the condition $\dot{t} > 0$ guarantees that the geodesic is future directed. For Kerr a suitable condition is to require that $g(\dot{\gamma}, e_0) \leq 0$ is satisfied. From that we obtain the condition for causal geodesic in the exterior region to be future directed to be:

$$E \geq \omega(r)L_z. \tag{3.4}$$

In terms of the conserved quotients this condition takes the form:

$$\operatorname{sgn}(L_z) = \begin{cases} +1 & \text{if } \mathcal{E} > \omega(r) \\ -1 & \text{if } \mathcal{E} < \omega(r) \\ \text{undet.} & \text{if } \mathcal{E} = \omega(r) \end{cases} \tag{3.5}$$

which eventually allows us to represent the pseudo potential, which will be introduced in the next subsection, for the co-rotating and the counter-rotating geodesics in the same plot.

3.1. The Radial Equation.

In this section we characterize the radial motion by locating the turning points of a geodesic in r direction. Turning points are characterized by the fact that the component of the tangent vector $\dot{\gamma}$ in the radial direction satisfies $\dot{r} = 0$. From equation (3.1c) we see immediately that the radial turning points are given by the zeros of the radial function R. In the following we will investigate the existence and location of these zeros. In this section we will be working

[3] The radial and the angular equation can be entirely decoupled by introducing a new non-affine parameter κ for the geodesics. It is defined by $\frac{\mathrm{d}\kappa}{\mathrm{d}\lambda} = \frac{1}{\Sigma}$.

with the conserved quantity Q as it is well suited to describe the phenomena we are interested here, namely the trapping and the null geodesics with negative energy.

Lemma 3. *$R(r, E, L_z, Q)$ is strictly positive in the exterior region for $Q < 0$.*

Proof. The radial function can be written as:

$$R(r, E, L_z, Q) = E^2 r^4 + (a^2 E^2 - Q - L_z^2) r^2 + 2MKr - a^2 Q, \tag{3.6}$$

which is clearly positive for large r. For the proof we make use of the Descartes rule, which states that if the terms of a polynomial with real coefficients are ordered by descending powers, then the number of positive roots is either equal to the number of sign differences between consecutive nonzero coefficients, or is less than it by an even number. Powers with zero coefficient are omitted from the series. For a proof of Descartes rule see for example [5, p.172]. Applied to (3.6) with $Q < 0$ we get that for two zeros of R to exist in $r \in (0, \infty)$ the conserved quantities of the geodesic have to satisfy the inequality:

$$a^2 E^2 - Q - L_z^2 < 0. \tag{3.7}$$

Otherwise there are no zeros at all and the proposition is true. Assume the contrary. Then for geodesics with certain parameters to exist at a given point, additionally to $R \geq 0$ we also need to have that $\Theta \geq 0$. Applying this condition to equation (3.1d) and combining it with inequality (3.7) we obtain the following estimate:

$$-\cos^4\theta a^2 E^2 \geq -Q > 0. \tag{3.8}$$

This is clearly a contradiction. □

Lemma 3 tells us that geodesics with $Q < 0$ either come from past null infinity $\mathcal{I}^-$ and cross the future event horizon $\mathcal{H}^+$ or come out of the past event horizon $\mathcal{H}^-$ and go to future null infinity $\mathcal{I}^+$. We will discuss the property of these geodesics in section 4.1. For the rest of this section we will restrict to the case of $Q \geq 0$. Note that even though some of the discussions and proofs might be simpler when working with $\mathcal{K}$ we are going to work with $\mathcal{Q}$ for all discussions that feed into the plot in section 6. This seems to be the natural choice to describe trapping and the ergoregion in phase space.

To find the essential properties of the radial motion, we use pseudo potentials. The pseudo potential $V(r, \mathcal{Q})$ is defined as the value of $\mathcal{E}$ such that the radius r is a turning point. In other words it is a solution to the equation:

$$R(r, V(r, \mathcal{Q}), 1, \mathcal{Q}) = \Sigma^2 \dot{r}^2 = 0. \tag{3.9}$$

This equation is quadratic in $V(r, \mathcal{Q})$ and for non-negative $\mathcal{Q}$ there exist two real solutions at every radius, denoted by $V_\pm$. They are given by:

$$V_\pm(r, \mathcal{Q}) = \frac{2Mar \pm \sqrt{r\Delta((1+\mathcal{Q})r^3 + a^2\mathcal{Q}(r+2M))}}{r[r(r^2+a^2)+2Ma^2]}. \tag{3.10}$$

Remark 4. *The pseudo potentials should not be mistaken for potentials known from classical mechanics, where the equation of motion is given by $\frac{1}{2}\dot{x}^2 + V(x) = E$. However the potentials of classical mechanics can always be considered as pseudo potentials in the above sense.*

The radial function can be rewritten as:

$$R(r, \mathcal{E}, 1, \mathcal{Q}) = L_z^2 r[r(r^2+a^2)+2Ma^2]\left(\mathcal{E} - V_+(r, \mathcal{Q})\right)\left(\mathcal{E} - V_-(r, \mathcal{Q})\right). \tag{3.11}$$

This form of R reveals the significance of the pseudo potentials: The only turning points that can exist for fixed $\mathcal{Q} > 0$ are those where either $\mathcal{E} = V_+(r, \mathcal{Q})$ or $\mathcal{E} = V_-(r, \mathcal{Q})$. Analyzing the properties of the $V_\pm$ allows us to extract all the information we are interested in.

First we note that for r big enough we have that $V_+ > 0$ and $V_- < 0$ for all $\mathcal{Q} \geq 0$. However in the limit we have that:

$$\lim_{r\to\infty} V_\pm = 0. \tag{3.12}$$

At the horizon the limit of the pseudo potential and its derivative are given by:

$$\lim_{r\to r_+} V_\pm(r) = \omega_H \tag{3.13}$$

$$\lim_{r\to r_+} \frac{dV_\pm}{dr}(r) = \pm\infty. \tag{3.14}$$

Lemma 5. *For a fixed value of $\mathcal{Q}$ the pseudo potentials $V_\pm(r, \mathcal{Q})$ have exactly one extremum as a function of r in the interval (r_+, ∞).*

Proof. It is clear from the above properties that V_+ (V_-) has at least one maximum (minimum) in the DOC. From the fact that the two pseudo potentials have the same limiting value at ∞ and at r_+ together with (3.11) we get that in both limits we have that $R(r, \mathcal{E}, 1, \mathcal{Q}) \geq 0$. Therefore $R(r, \mathcal{E}, 1, \mathcal{Q})$ has to have an even number of zeros in the interval (r_+, ∞). Given the fact that $R(r, \mathcal{E}, 1, \mathcal{Q})$ is a fourth order polynomial it can have at most 4 zeros. From the asymptotic behaviour of the potentials $V_\pm$ we get that they need to have an odd number of extrema. Therefore if for some value of $\mathcal{Q}$ one of the potentials has more than one extremum there exists $\mathcal{E}$ such that $R(r, \mathcal{E}, 1, \mathcal{Q})$ has three zeros in $r \in (r_+, \infty)$. Applying Descartes rule to (3.1c) we infer that $R(r, \mathcal{E}, 1, \mathcal{Q})$ can have at most three zeros in $r \in [0, \infty)$. But $R(0, \mathcal{E}, 1, \mathcal{Q}) \leq 0$ and $R(r_+, \mathcal{E}, 1, \mathcal{Q}) \geq 0$. Hence there is at least one zero of $R(r, \mathcal{E}, 1, \mathcal{Q})$ in the interval $[0, r_+]$, so it is impossible for $R(r, \mathcal{E}, 1, \mathcal{Q})$ to have three zeros in (r_+, ∞). From that it follows that $V_\pm$ can both only have one extremum in that interval. □

Stationary points occur at the extrema of the pseudo potentials. So Lemma 5 tells us that for every fixed value of $\mathcal{Q} \geq 0$ there exist exactly two spherical geodesics with radii $r = r^\pm_{trap}$ and energies $\mathcal{E}_{trap\pm} = V_\pm(r^\pm_{trap})$. They will be studied in depth in section 4.2. Bounded geodesics with non-constant r would only be possible between two extrema of one of the pseudo potentials. These are excluded by the Lemma.
From (3.1c) we have that for any geodesics to exist we have to have $R(r, \mathcal{E}, 1, \mathcal{Q}) \geq 0$. This condition is satisfied except if $V_-(r, \mathcal{Q}) < \mathcal{E} < V_+(r, \mathcal{Q})$. This set is therefore a forbidden region in the $(r, \mathcal{E})$ plane. Furthermore it follows that $R(r, \mathcal{E}, 1, \mathcal{Q}) \leq 0$ for $\mathcal{E} = \omega(r)$ with equality only in the limits $r \to r_+$ and $r \to \infty$. Therefore we have that:

$$V_-(r) \leq \omega(r) \leq V_+(r). \tag{3.15}$$

Again, the equality can occur only at the horizon and in the limit $r \to \infty$. This fact combined with (3.5) shows that for future pointing null geodesics

$$\mathrm{sgn}(L_z) = \begin{cases} +1 & \text{if } \mathcal{E} \geq V_+(r), \\ -1 & \text{if } \mathcal{E} \leq V_-(r). \end{cases} \tag{3.16}$$

Therefore the pseudopotential V_+ determines the behaviour of co-rotating null geodesics and V_- that of counter-rotating ones. Furthermore it is worth noting that $\mathcal{E} \geq V_+(r)$ implies $E > 0$. Finally we observe that for every fixed radius $r \geq r_+$ we get from inspection of (3.10) that:

$$\frac{\partial V_-}{\partial \mathcal{Q}} \leq 0 \leq \frac{\partial V_+}{\partial \mathcal{Q}} \tag{3.17}$$

holds. The equality in the relation occurs again only in the limits $r \to r_+$ and $r \to \infty$. This means that for every radius $r > r_+$ the range of forbidden values of $\mathcal{E}$ is strictly expanding as $\mathcal{Q}$ increases. This fact will be quite useful for the considerations in section 4.2.

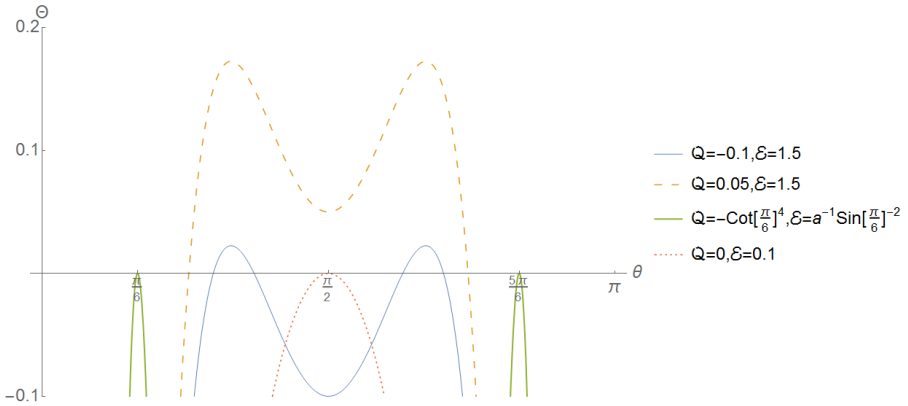

FIGURE 1. This figure shows shapes of function $\frac{\Theta}{L_z^2}$ for four choices of values of conserved quotients.

3.2. **The θ Equation.** In Schwarzschild spacetimes, due to spherical symmetry the motion of any geodesics is contained in a plane. This means that for every geodesic there exists a spherical coordinate system in which it is constrained to the equatorial plane $\theta = \frac{\pi}{2}$. This is no longer true in Kerr spacetimes, but most geodesics are still constrained in θ direction. The allowed range of θ is obtained by solving the inequality $\Theta(\theta, E, L_z, Q) \geq 0$. After multiplication with $\sin^2(\theta)$, $\Theta(\theta, E, L_z, Q)$ can be expressed as a quadratic polynomial in the variable $\cos^2(\theta)$. Hence $\Theta(\theta, E, L_z, Q) = 0$ has two solutions given by:

$$\cos^2 \theta_{turn} = \frac{a^2E^2 - L_z^2 - Q \pm \sqrt{(a^2E^2 - L_z^2 - Q)^2 + 4a^2E^2Q}}{2a^2E^2}. \tag{3.18}$$

For $Q > 0$ only the solution with the plus sign is relevant and the motion will always be contained in a band $\theta_{min} < \theta_{eq} < \theta_{max}$ symmetric about the equator $\theta_{eq} = \frac{\pi}{2}$. As $|L_z|$ increases, this band shrinks. In fact only in the case $L_z = 0$ it is possible for a geodesic to reach the poles $\theta = 0$, $\theta = \pi$. Otherwise $\Theta(\theta, E, L_z, Q)$ blows up to $-\infty$ there. If $Q < 0$ both solutions are positive and the inclination of the geodesic with respect to the equator is also constrained away from the equator, so either $\theta_{eq} < \theta_{min} < \theta_{max}$ or $\theta_{eq} > \theta_{max} > \theta_{min}$. These trajectories will be contained in a disjoint band which intersects neither the equator nor the pole. This band can degenerate to a point, i.e. there exist null geodesics which stay at $\theta = \text{const}$. The relevance of these trajectories and how they are connected to the Schwarzschild case will be discussed in the next section. All possibilities for the potentials that constrain the motion in θ direction are summarized in the Figure 1.

4. Special Geodesics

We will now apply the discussions of the last section to describe a number of special geodesics in Kerr geometries. All of these are in some way related to either the black hole stability problem or the black hole uniqueness problem.

4.1. **Radially In-/Out-going Null Geodesics.** In this section we find geodesics which generalize the radially ingoing and outgoing congruences in Schwarzschild spacetimes. In section 3.1 we saw that the geodesics with $Q < 0$ extend from the horizon to infinity. In section 3.2 we saw that $Q < 0$ is again a special case, as these null geodesics can never intersect the equator and in the extreme case are even constrained to a fixed value of θ. At first this behaviour seems odd, but a similar situation can be observed in Schwarzschild. If we look at geodesics which move in a plane with inclination θ_0 about the equatorial plane we see that there exists a set of

null geodesics with similar properties as the ones with $Q < 0$ in Kerr. It is clear that the radially ingoing geodesic which moves orthogonally to the axis around which the plane of motion was rotated, moves at fixed θ value, namely that at which the plane is inclined with respect to the equatorial plane, hence $\theta = \pi/2 \pm \theta_0$. Furthermore some null geodesics reach the horizon before intersecting the equatorial plane. They don't necessarily move at fixed θ but their motion in θ direction is still constrained away form the equatorial plane and away from the poles of the coordinate system. Now we want to investigate the null geodesics which move at fixed θ in Kerr. Demanding that θ = const. is equivalent to requiring $\Theta = \frac{d}{d\theta}\Theta = 0$. From these conditions we obtain:

$$L_z = \pm aE \sin^2\theta, \tag{4.1a}$$

$$Q = -a^2E^2\cos^4\theta, \tag{4.1b}$$

$$K = 0. \tag{4.1c}$$

By choosing the plus sign for L_z in the above equation, it follows from the remaining equations of motion that:

$$\frac{\dot{\phi}}{\dot{t}} = \frac{d\phi}{dt} = \omega(r), \tag{4.2a}$$

$$\frac{\dot{r}}{\dot{t}} = \frac{dr}{dt} = \pm\frac{\Delta}{r^2+a^2}. \tag{4.2b}$$

This congruence is generated by the principal null directions $e_0 \pm e_1$. When choosing the minus sign for L_z in (4.1) the remaining equations of motions can not be simplified in a similar manner. In the case $a = 0$ these are the radially in-/outgoing null geodesics. An interesting observation is that along these geodesics the inner product of the $(\partial_t)^\mu$ vector field is monotone. A simple calculation shows that:

$$\dot{\gamma}^\mu\nabla_\mu((\partial_t)^\nu(\partial_t)_\nu) = \dot{r}\frac{2M(r^2 - a^2\cos^2\theta)}{\Sigma^2} + \dot{\theta}\frac{2Ma^2 r\sin 2\theta}{\Sigma^2}. \tag{4.3}$$

For the principal null congruence we have $\dot{\theta} = 0$, the coefficient of $\dot{r}$ is positive and there is no turning point in r. This property might be interesting in the context of the black hole uniqueness problem. If one could show a similar monotonicity statement for a congruence of null geodesics in general stationary black hole spacetimes, one could conclude that the ergosphere in such spacetimes has only one connected component enclosing the horizon. This is a necessary condition if one wants to show that no trapped **T**-orthogonal null geodesics can exist in that case.

4.2. **The Trapped Set.** One of the most important features of geodesic motion in black hole spacetimes is the possibility of trapping. A geodesic is called trapped if its motion is bounded in a spatially compact region away from the horizon. In Kerr this corresponds to the geodesics motion being bounded in r direction. This is only possible if r = const. or if the motion is between two turning points of the radial motion. For null geodesics in Kerr we ruled out the second option in Lemma 5. We will now discuss orbits of constant radius.[4] These null geodesics are stationary points of the radial motion, hence null geodesics with $\dot{r} = \ddot{r} = 0$. Dividing equation (3.1c) by Σ and taking the derivative with respect to λ we see that this condition is equivalent to $R(r) = \frac{d}{dr}R(r) = 0$. The solutions to these equations can be parametrized explicitly by, cf. [19]:

$$\mathcal{E}_{trap}(r) = -\frac{a(r-M)}{A(r)} = \omega(r)\left(1 - \frac{2r\Delta}{A(r)}\right) \tag{4.4}$$

[4]Null geodesics of constant radius are often referred to as "spherical null geodesics" but it is important to note that r = const. does not imply that the whole sphere is accessible for such geodesics.

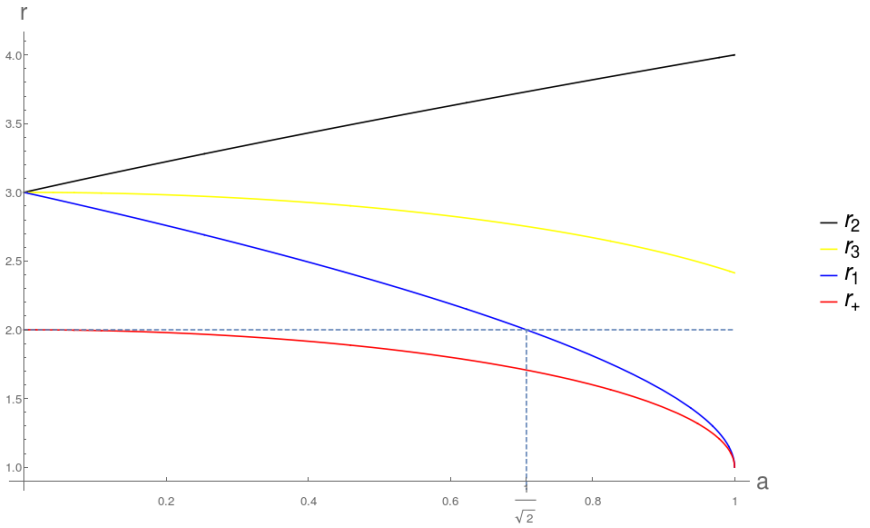

FIGURE 2. Plot of the relation between the radius of the equatorial trapped null geodesics at r_1 and r_2, the trapped null geodesic with $L_z = 0$ at r_3 and the horizon at r_+ for all values of a.

$$\mathcal{Q}_{trap}(r) = -\frac{B(r)}{A^2(r)} \tag{4.5}$$

$$A(r) = r^3 - 3Mr^2 + a^2 r + a^2 M = (r - r_3)P_2(r) \tag{4.6}$$

$$B(r) = r^3(r^3 - 6Mr^2 + 9M^2 r - 4a^2 M) = (r - r_1)(r - r_2)P_4(r) \tag{4.7}$$

where P_2 and P_4 are polynomials in r, quadratic and quartic respectively, which are strictly positive in the DOC. The following three radii are particularly important:

$$r_1 = 2M\left(1 + \cos\left(\frac{2}{3}\arccos\left(-\frac{a}{M}\right)\right)\right) \tag{4.8}$$

$$r_2 = 2M\left(1 + \cos\left(\frac{2}{3}\arccos\left(\frac{a}{M}\right)\right)\right) \tag{4.9}$$

$$r_3 = M + 2\sqrt{M^2 - \frac{a^2}{3}}\cos\left(\frac{1}{3}\arccos\left(\frac{M(M^2 - a^2)}{(M^2 - \frac{a^2}{3})^{\frac{3}{2}}}\right)\right) \tag{4.10}$$

satisfying the inequalities:

$$M < r_+ < r_1 < r_3 < r_2 < 4M \tag{4.11}$$

for $a \in (0, M)$. Orbits of constant radius are allowed only inside the interval $[r_1, r_2]$, because outside of it Q would have to be negative. This possibility has already been excluded in Lemma 3. The boundaries of the interval at $r = r_1$ and $r = r_2$ correspond to circular geodesics constrained to the equatorial plane with $Q = 0$. The trapped null geodesics at $r = r_3$ have $L_z = 0$ which is the reason why the functions $\mathcal{E}_{trap}$ and $\mathcal{Q}_{trap}$ blow up there. From the second representation in (4.4) we see that $\mathcal{E}_{trap}(r) - \omega(r)$ is positive in $[r_1, r_3)$ and negative in $(r_3, r_2]$. Combined with (3.16) this implies that the stationary points in $[r_1, r_3)$ correspond to extrema of V_+ and the stationary points in $(r_3, r_2]$ correspond to extrema of V_-. In Lemma 5 we showed that V_+ and V_- both have exactly one extremum. Since extrema of the pseudo potentials always correspond to orbits of constant radius, we get that the extrema of $V_+(r, \mathcal{Q})$ and $V_-(r, \mathcal{Q})$ have to be within the intervals $[r_1, r_3)$ and $(r_3, r_2]$ respectively for any value of $\mathcal{Q}$. In Figure 2 we plot the behaviour of these intervals as a function of a/M.

We now know that the maps given by:

$$[0,\infty) \ni \mathcal{Q} \mapsto r^{+}_{trap} \in [r_1, r_3)$$

$$[0,\infty) \ni \mathcal{Q} \mapsto r^{-}_{trap} \in (r_3, r_2]$$

which take $\mathcal{Q}$ into radii of trapped geodesics corresponding to the unique maximum of $V_+(r,\mathcal{Q})$ and minimum of $V_-(r,\mathcal{Q})$ respectively are one-to-one and therefore monotone. By using (4.5) the sign of their derivatives can be easily evaluated in some ϵ-neighbourhood of $r = r_3$ where the term of highest order in $\frac{1}{r-r_3}$ dominates:

$$\frac{\partial r^{-}_{trap}}{\partial \mathcal{Q}} < 0 < \frac{\partial r^{+}_{trap}}{\partial \mathcal{Q}}. \tag{4.12}$$

By the equation (3.17) and the fact that radii of trapping always correspond to global extrema of the pseudo potentials we get that:

$$\frac{\partial}{\partial \mathcal{Q}} \mathcal{E}_{trap}(r^{-}_{trap}(\mathcal{Q})) < 0 < \frac{\partial}{\partial \mathcal{Q}} \mathcal{E}_{trap}(r^{+}_{trap}(\mathcal{Q})). \tag{4.13}$$

Using the chain rule and combining these two facts we obtain:

$$\frac{\partial \mathcal{E}_{trap}}{\partial r} > 0. \tag{4.14}$$

These inequalities provide an important piece of the picture of the influence of $\mathcal{Q}$ on the trapped geodesics. We have $\mathcal{Q} = 0$ for the outermost circular geodesics and as we increase it, the radii of trapping converge towards $r = r_3$ while $\mathcal{E}$ blows up to $\pm\infty$, with the sign depending on the direction from which we approach r_3. We can also desciribe the function $\mathcal{E}_{trap}(r)$: it starts with some finite positive value at $r = r_1$ and increases monotonically to $+\infty$ as r approaches r_3. There it jumps to $-\infty$ and increases again to a finite negative value at $r = r_2$.
It is interesting to ask what region in physical space is accessible for trapped geodesics. By plugging (4.5) and (4.4) into the equation $\Theta = 0$ we get that for a geodesic with $r = \text{const.}$:

$$\cos^2\theta_{turn} = \frac{2\sqrt{Mr^2\Delta(2r^3 - 3Mr^2 + a^2M)} - r(r^3 - 3M^2r + 2a^2M)}{a^2(r-M)^2} \tag{4.15}$$

holds. This gives two turning points in θ direction which are symmetric about the equatorial plane. The whole region of trapping in the (r,θ) plane is bounded by curves defined implicitly by (4.15) and $r_1 \le r \le r_2$. Figure (3) presents this set for a particular value of a.

Remark 6. *Two warnings:*

1. *One has to be careful when interpreting Figure 3 (and the plots in the Mathematica notebook). Despite the fact that the region in physical space occupies finite range of r values, every individual trapped null geodesic is still constrained to a fixed radius. For an insight on what those trajectories look like in detail we recommend the study of* [19].
2. *When taking $a \to M$ in the Mathematica notebook the ergosphere appears to develop a kink on the rotation axis. This is an artifact of the coordinate system, as the ergosphere coincides with the horizon there and is thus orthogonal to itself.*

4.3. **T-Orthogonal Null Geodesics.** In the ergoregion there exist null geodesics with negative values of E. In physical space they are constrained to the region defined by equation (2.20). From Lemma 3 we know that geodesics with $Q < 0$ reach either $\mathcal{I}^+$ or come from $\mathcal{I}^-$ and can therefore not have negative values of E. This allows us to use the pseudo potentials to give a more precise characterization of the ergoregion in phase space. It is located in the region where $V_-(\mathcal{Q}) > 0$,

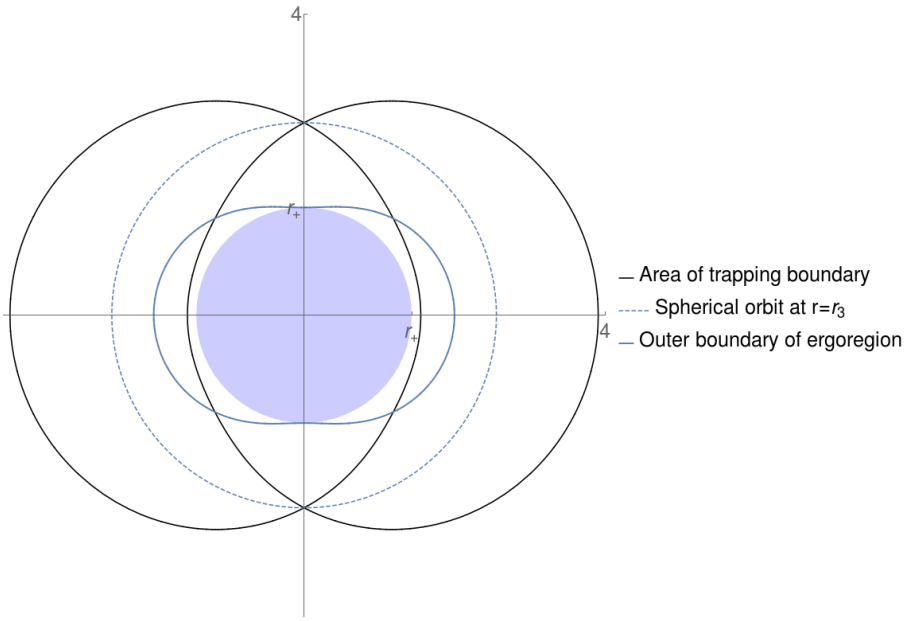

FIGURE 3. The region accessible for trapped null geodesics for $a = 0.902$. The shaded region represents the black hole, $r \leq r_+$. The only qualitative change in this picture occurs at $a = \frac{1}{\sqrt{2}}$ because at this value the region of trapping starts intersecting with the ergoregion.

between $\mathcal{E} = 0$ and $V_-(\mathcal{Q})$. An immediate consequence of that is, that all future pointing null geodesics with negative $\mathcal{E}$ begin at the past event horizon and end at the future event horizon. Furthermore they must have $L_z < 0$. Those null geodesics with $\mathcal{E} = 0$ can reach the boundary of the ergoregion. In this case equation (3.1d) gives us, that:

$$\mathcal{Q} = \frac{\cos^2(\theta_{max})}{\sin^2(\theta_{max})}. \tag{4.16}$$

When calculating the turning points from equation (3.1c) we get that:

$$\sin^2(\theta_{max}) R\left(r, 0, 1, \frac{cos^2(\theta_{max})}{sin^2(\theta_{max})}\right) = -r^2 + 2Mr - a^2 cos^2(\theta_{max}) = 0. \tag{4.17}$$

The only solution to this equation in the exterior region is:

$$r_{turn}(\theta_{max}) = M + \sqrt{M^2 - a^2 cos^2(\theta_{max})} \tag{4.18}$$

which is exactly the location of the ergo sphere (2.20). So $V_-(\mathcal{Q}) > 0$ can be considered as the boundary of the ergoregion in phase space. From this considerations we see immediately that **T**-orthogonal null geodesics are clearly non-trapped in Kerr. In fact there do not even exist any trapped null geodesics orthogonal to:

$$K^\nu = (\partial_t)^\nu + \epsilon_{min}(\partial_\phi)^\nu \tag{4.19}$$

where $\epsilon_{min} = min[|V_+(0, r_1)|, |V_-(0, r_2)|]$.

5. Trapping as a Set of Directions

In this section we will link the previous discussion to the black hole shadows. We introduce a more formal framework for the discussion. This allows us to give a more technical discussion of the trapped sets in Schwarzschild and Kerr black holes.

5.1. **Framework.** First we have to introduce the basic framework and notations. Let $\mathcal{M}$ be a smooth manifold with Lorenzian metric g. At any point p in $\mathcal{M}$ you can find an orthonormal basis (e_0, e_1, e_2, e_3) for the tangent space, with e_0 being the timelike direction. It is sufficient to treat only future directed null geodesics as the past directed ones are identical up to a sign flip in the parametrization. The tangent vector to any future pointing null geodesic can be written as:

$$\dot{\gamma}(k|_p)|_p = \alpha(e_0 + k_1 e_1 + k_2 e_2 + k_3 e_3) \tag{5.1}$$

where $\alpha = -g(\dot{\gamma}, e_0)$ and $k = (k_1, k_2, k_3)$ satisfies $|k|^2 = 1$, hence $k \in S^2$. The geodesic is independent of the scaling of the tangent vector as this corresponds to an affine reparametrization for the null geodesic. We will therefore set $\alpha = 1$ in the following discussion. The S^2 is often referred to as the celestial sphere of a timelike observer at p whose tangent vector is given by e_0, cf. [16, p.8].
For the further discussions we fix the tetrads. We can make the following definition:

Definition 7. *Let $\gamma(k|_p)$ denote a null geodesic through p for which the tangent vector at p is given by equation* (5.1).

It is clear that $\gamma(k_a|_p)$ and $\gamma(k_b|_p)$ are equivalent up to parametrization if $k_a = k_b$. Suppose now that $\mathcal{M}$ is the exterior region of a black hole spacetime with complete future and past null infinity $\mathcal{I}^{\pm}$ and a boundary given by the future and past event horizon $\mathcal{H}^+ \cup \mathcal{H}^-$. We can then define the following sets on S^2 at every point p.

Definition 8. *The future infalling set:* $\Omega_{\mathcal{H}^+}(p) := \{k \in S^2 | \gamma(k|_p) \cap \mathcal{H}^+ \neq \emptyset\}$.
The future escaping set: $\Omega_{\mathcal{I}^+}(p) := \{k \in S^2 | \gamma(k|_p) \cap \mathcal{I}^+ \neq \emptyset\}$.
The future trapped set: $\mathbb{T}_+(p) := \{k \in S^2 | \gamma(k|_p) \cap (\mathcal{H}^+ \cup \mathcal{I}^+) = \emptyset\}$.
The past infalling set: $\Omega_{\mathcal{H}^-}(p) := \{k \in S^2 | \gamma(k|_p) \cap \mathcal{H}^- \neq \emptyset\}$.
The past escaping set: $\Omega_{\mathcal{I}^-}(p) := \{k \in S^2 | \gamma(k|_p) \cap \mathcal{I}^- \neq \emptyset\}$.
The past trapped set: $\mathbb{T}_-(p) := \{k \in S^2 | \gamma(k|_p) \cap (\mathcal{H}^- \cup \mathcal{I}^-) = \emptyset\}$

We finish the section by defining the trapped set to be:

Definition 9. *The trapped set:* $\mathbb{T}(p) := \mathbb{T}_+(p) \cap \mathbb{T}_-(p)$.

The region of trapping in the manifold $\mathcal{M}$ is then given by:

Definition 10. *Region of trapping:* $\mathcal{A} := \{p \in \mathcal{M} | \mathbb{T}(p) \neq \emptyset\}$.

5.2. **The trapped sets in Schwarzschild.** The discussion of Schwarzschild serves as an easy example for the various concepts.

Definition 11. *We refer to the set $\Omega_{\mathcal{H}^-}(p) \cup \mathbb{T}_-(p)$ as the shadow of the black hole.*

However for any practical purposes information about its boundary which is given by $\mathbb{T}_-(p)$ is good enough. An observer in the exterior region can only observe light from background sources along directions in the set $\Omega_{\mathcal{I}^-}(p)$. From the radial equation we get immediately that if $k = (k_1, k_2, k_3) \in \mathbb{T}_+(p)$ then $k = (-k_1, k_2, k_3) \in \mathbb{T}_-(p)$. Hence the properties of the past and the future sets are equivalent. This is true both in Schwarzschild and Kerr.
An explicit formula for the shadow of a Schwarzschild black hole was first given in [18]. In Schwarzschild the orthonormal tetrad (2.6) reduces to:

$$\begin{aligned} e_0 &= \frac{1}{\sqrt{1-2M/r}}\partial_t, & e_1 &= \sqrt{1-2M/r}\partial_r, \\ e_2 &= \frac{1}{r}\partial_\theta, & e_3 &= \frac{1}{r\sin\theta}\partial_\phi. \end{aligned} \tag{5.2}$$

To determine the structure of $\mathbb{T}_\pm(p)$ in Schwarzschild it is sufficient to consider p in the equatorial plane and $k = (\cos\Psi, 0, \sin\Psi)$ with $\Psi \in [0, \pi]$. The entire sets $\mathbb{T}_\pm(p)$ are then obtained by rotating around the e_1 direction. Note that from

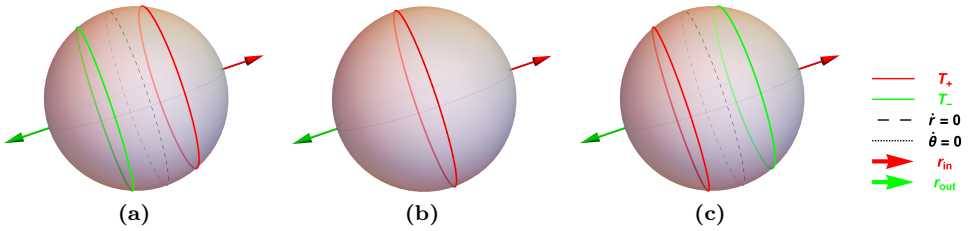

FIGURE 4. The trapped set on the celestial sphere of a standard observer at different radial location in a Schwarzschild DOC. Observer (a) is located outside the photon sphere at $r = 3.9M$, observer (b) is located on the photon sphere at $r = 3M$ and finally observer(c) is located between the horizon and the photonsphere at $r = 2.5M$. One can see that the future trapped set moves from the ingoing hemisphere in (a) to the outgoing hemisphere in (c) as one varies the location of the observer. The future and past trapped set coincide on the $\dot{r} = 0$ line when the observer is located on the photon sphere at $r = 3M$ in (b)

the tetrad it is obvious that $E(k) = E(r)$ is independent of Ψ. On the other hand $L_z(k)$ is zero for $\Psi = \{0, \pi\}$ and maximal for $\Psi = \pi/2$. Away from that maximum, L_z is a monotone function of Ψ. Note that the geodesic that corresponds to $\Psi = \pi/2$ has $k_1 = 0$ and thus a radial turning point. Thus the E/L_z value of this geodesic corresponds to the minimum value any geodesic can have at this point in the manifold. For $r \neq 3M$ this is smaller then the value of trapping and thus there exist two k with the property that $E/L_z(k) = 1/\sqrt{27M^2}$. One of them has $k_1 > 0$ and therefore $\dot{r} > 0$ and one has $\dot{r} < 0$. For $r > 3M$ the first corresponds to $\mathbb{T}_-(p)$ and the second corresponds to $\mathbb{T}_+(p)$. For $2M < r < 3M$ the roles are reversed. For $r = 3M$ we have $\mathbb{T}_+(p) = \mathbb{T}_-(p) = (0, k_2, k_3)$. In Figure 4 we depict these three cases for some fixed radii. To conclude we see that $\mathbb{T}_+(p)$ and $\mathbb{T}_-(p)$ are circles on the celestial sphere independent of the value of $r(p)$. In [16, p.14] it is shown that Lorentz transformations on the observer correspond to conformal transformations on the celestial sphere. They are equivalent up to Möbius transformations on the complex plane when considering the S_2 to be the Riemann sphere. Hence circles on the celestial sphere stay circles under Lorentz transformations. As a consequence if $r(p_a) \neq r(p_b)$ then there exists a Lorentz transformation (**LT**) such that $\mathbb{T}_-(p_a) = \mathbf{LT}[\mathbb{T}_-(p_b)]$. This concept is sufficiently important that it deserves a proper definition.

Definition 12. *The shadows at two points p_1, p_2 are called degenerate if, upon identification of the two celestial spheres by the orthonormal basis, there exists an element of the conformal group on S^2 that transforms $\mathbb{T}_-(p_1)$ into $\mathbb{T}_-(p_2)$.*

Remark 13. *The shadow at two points p_1, p_2 being degenerate implies that for every observer at p_1 there exists an observer at p_2 for which the shadow on S^2 is identical. Because this notion compares structures on S^2, the two points do not have to be in the same manifold for their shadows to be degenerate. Just from the shadow alone an observer can not distinguish between these two configurations.*

The only reliably information an observer can obtain is thus, that $\mathbb{T}_-(p)$ is a proper circle on his celestial sphere.

5.3. **The trapped sets in Kerr.** We will now discuss the properties of the sets $\mathbb{T}_\pm(p)$ in Kerr. Note that the equations of motion for r (3.1c) and θ (3.1d) have two solutions that differ only by a sign for a fixed combination of E, L_z, K. Therefore

we know that the trapped sets will have a reflection symmetry across the $k_1 = 0$ and the $k_2 = 0$ planes. A sign change in k_2 maps both sets $\mathbb{T}_{\pm}(p)$ to themselves, while a sign flip in k_1 maps $\mathbb{T}_{+}(p)$ to $\mathbb{T}_{-}(p)$ and vice versa.
In the following we will use the parametrization of [10]. We introduce the coordinates $\rho \in [0, \pi]$ and $\psi \in [0, 2\pi)$ on the celestial sphere. Thus (5.1) can be written as:

$$\dot{\gamma}(\rho, \psi)|_p = \alpha(e_0 + \cos(\rho)e_1 + \sin(\rho)\cos(\psi)e_2 + \sin(\rho)\sin(\psi)e_3) \tag{5.3}$$

The direction towards the black hole is given by $\rho = \pi$. Following [10] one finds the following parametrization of the celestial sphere in terms of constants of motion:

$$\sin(\psi) = \left.\frac{(\mathcal{L} - a) + a\cos^2(\theta)}{\sqrt{\mathcal{K}}\sin(\theta)}\right|_p, \tag{5.4a}$$

$$\sin(\rho) = \left.\frac{\sqrt{\Delta\mathcal{K}}}{r^2 - a(\mathcal{L} - a)}\right|_p, \tag{5.4b}$$

Analog to the functions (4.4) and (4.5) which give the value of the conserved quantities in terms of the radius of trapping, we can give such relations for the conserved quotients $\mathcal{K}$ and $\mathcal{L}$ in this formulation they can be found for example in [10]. To differ between the trapped radius and the observers radius we use $x \in [r_{min}(\theta), r_{max}(\theta)]$ to parametrize the conserved quantities of the trapped set. Here $r_{min}(\theta)$ and $r_{max}(\theta)$ are given as the intersection of a cone of constant θ with the boundary of the area of trapping. Note that it is part of the following proof to show that the given interval is in fact the correct domain for the parameter x. The parameter x here corresponds to the radius of the trapped null geodesic which a particular future trapped direction is asymptoting to. We have then:

$$\mathcal{K} = \frac{16x^2\Delta(x)}{(\Delta'(x))^2} \tag{5.5a}$$

$$a(\mathcal{L} - a) = \left(x^2 - \frac{4x\Delta(x)}{\Delta'(x)}\right) \tag{5.5b}$$

where $\Delta'(x) = 2x - 2M$ is the partial derivative of $\Delta(x)$ with respect to x .Plugging (5.5) into (5.4) we obtain:

$$\sin(\psi) = \frac{\Delta'(x)\{x^2 + a^2\cos^2(\theta(p))\} - 4x\Delta(x)}{4x\sqrt{\Delta(x)}a\sin(\theta(p))} \tag{5.6a}$$

$$\sin(\rho) = \frac{4x\sqrt{\Delta(r(p))\Delta(x)}}{\Delta'(x)(r(p)^2 - x^2) + 4x\Delta(x)} := h(x) \tag{5.6b}$$

We are now ready to prove the following Theorem.

Theorem 14. *The sets $\mathbb{T}_{+}(p)$ and $\mathbb{T}_{-}(p)$ are smooth curves on the celestial sphere of any timelike observer at any point in the exterior region of any subextremal Kerr spacetime.*

Proof. We start by anayzing the right hand side of (5.6a):

$$\begin{aligned}\frac{d}{dx}\left(\frac{\Delta'(x)\{x^2 + a^2\cos^2(\theta(p))\} - 4x\Delta(x)}{4x\sqrt{\Delta(x)}a\sin(\theta(p))}\right) \\ = \frac{\{x^2 + a^2\cos^2(\theta(p))\}((M-x)^3 - M(M^2 - a^2))}{2x^2\Delta(x)^{3/2}a\sin(\theta(p))},\end{aligned} \tag{5.7}$$

which is strictly negative for $x \in (r_+, \infty)$. The limit of the right hand side of (5.6a) is given by ∞ for $x \to r_+$ and $-\infty$ for $x \to \infty$. Therefore the right hand side is invertible and $x(\sin(\psi))$ is a smooth function of ψ with extrema at the extremal points of $\sin(\psi)$. As was shown in [10] the minimum $x_{min}(\theta(p))$ at $\psi = \pi/2$ and the maximum of $x_{max}(\theta(p))$ at $\psi = 3\pi/2$ correspond exactly to the intersections

of a cone with constant θ with the boundary of the region of trapping. This can be seen by setting the left hand side of (5.6a) equal to ± 1, taking the square of the equation, solving for $\cos^2(\theta)$ and comparing to (4.15). Important here is that $[x_{min}(\theta(p)), x_{max}(\theta(p))] \subset [r_1, r_2]$ for all values of $\theta(p)$. Now we take a look at the right hand side of equation (5.6b):

$$\frac{d}{dx}\left(h(x)\right) = \frac{8(r(p)^2 - x^2)\Delta(r(p))((x-M)^3 + M(M^2 - a^2))}{\sqrt{\Delta(r(p))\Delta(x)}(4x\Delta(x) + (r(p)^2 - x^2)\Delta'(x))^2}. \tag{5.8}$$

This is positive when $x < r(p)$ and negative when $x > r(p)$. The denominator never vanishes for $x \in (r_+, \infty)$ because:

$$(4x\Delta(x) + (r(p)^2 - x^2)\Delta'(x))|_{\{r(p)=r_+, x=r_+\}} = 0 \tag{5.9}$$

and

$$\frac{d}{dx}(4x\Delta(x) + (r(p)^2 - x^2)\Delta'(x)) = 2(3x^2 - 6Mx + 2a^2 + r(p)^2) > 0 \tag{5.10}$$

$$\frac{d}{dr(p)}(4x\Delta(x) + (r(p)^2 - x^2)\Delta'(x)) = 2r(p)\Delta'(x) > 0, \tag{5.11}$$

where we used $r(p) > r_+ > M > a$ in (5.10).
If we set $x = r(p)$ in (5.6b) then the right hand side is equal to 1. Furthermore in any of the limits $r(p) \to r_+$, $r(p) \to \infty$, $x \to r_+$, and $x \to \infty$ it goes to zero.

Case 1. *If $p \notin \mathcal{A}$ hence if $r(p) \notin [x_{min}(\theta(p)), x_{max}(\theta(p))]$ then the two functions:*

$$\rho_1(\psi) = \arcsin(h(x(\psi))) : [0, 2\pi) \to [\rho_{1_{min}}, \rho_{1_{max}}] \subset \left(0, \frac{\pi}{2}\right) \tag{5.12}$$

$$\rho_2(\psi) = \pi - \arcsin(h(x(\psi))) : [0, 2\pi) \to [\rho_{2_{min}}, \rho_{2_{max}}] \subset \left(\frac{\pi}{2}, \pi\right) \tag{5.13}$$

are both smooth with $\rho_1(0) = \rho_1(2\pi)$ and $\rho_2(0) = \rho_2(2\pi)$. If p is between the region of trapping and the asymptotically flat end, the function $\rho_2(\psi)$ corresponds to $\mathbb{T}_+(p)$ and $\rho_1(\psi)$ corresponds to $\mathbb{T}_-(p)$. Because $(\pi/2, \pi]$ corresponds to the geodesic with $\dot{r} < 0$. If p is between the region of trapping and the horizon then the role of $\rho_1(\psi)$ and $\rho_2(\psi)$ are switched.

Case 2. *If $p \in \mathcal{A}$ we need to do some extra work. For simplicity we only consider the interval $\psi \in [\pi/2, 3\pi/2]$ as the rest follows by symmetry of $\sin(\psi)$ in $[0, \pi]$ across $\pi/2$ and in $[\pi, 2\pi]$ across $3\pi/2$. Let $\arcsin(x)$ map into this interval, then we define:*

$$\psi_0(r(p)) = \arcsin\left(\frac{\Delta'(r(p))\{r(p)^2 + a^2\cos^2(\theta(p))\} - 4r(p)\Delta(r(p))}{4r(p)\sqrt{\Delta(r(p))}a\sin(\theta(p))}\right). \tag{5.14}$$

The two functions:

$$\rho_3(\psi) = \begin{cases} \arcsin(h(x(\psi))) & \text{if } \psi \in [\pi/2, \psi_0(r(p))] \\ \pi - \arcsin(h(x(\psi))) & \text{if } \psi \in (\psi_0(r(p)), 3\pi/2] \end{cases} \tag{5.15}$$

$$\rho_4(\psi) = \begin{cases} \pi - \arcsin(h(x(\psi))) & \text{if } \psi \in [\pi/2, \psi_0(r(p))] \\ \arcsin(h(x(\psi))) & \text{if } \psi \in (\psi_0(r(p)), 3\pi/2] \end{cases} \tag{5.16}$$

are then smooth on $[\pi/2, 3\pi/2]$. For a proof see Appendix A and note that at ψ_0, $h(x(\psi))$ satisfies the conditions required in the appendix. Since $p \in \mathcal{A}$ we have that $x_{min}(\theta(p)) < r(p) < x_{max}(\theta(p))$. Therefore the geodesic on the celestial sphere parametrized by $x_{max}(\theta(p))$ has to have $\dot{r} > 0$ and thus has to be in $[0, \pi/2)$. On the other hand the geodesic on the celestial sphere parametrized by $x_{min}(\theta(p))$ has to have $\dot{r} < 0$ and thus has to be in $(\pi/2, \pi]$. In fact by the monotonicity of the right hand side of (5.6a) and the fact that $x(\psi_0) = r(p)$ we know that for $\psi \in [\pi/2, \psi_0)$ we have $x(\psi) < r(p)$ and for $\psi \in (\psi_0, 3\pi/2]$ we have $x(\psi) > r(p)$. Thus we can conclude that for $p \in \mathcal{A}$, ρ_4 corresponds to $\mathbb{T}_+(p)$ and ρ_3 corresponds to $\mathbb{T}_-(p)$ and thus both sets are smooth.

Case 3. *In the special case when* $r(p) = x_{max}(\theta(p))$ *or* $r(p) = x_{min}(\theta(p))$ *the functions* ρ_1 *and* ρ_2 *describing* $\mathbb{T}_{\pm}(p)$ *do reach* $\rho = \pi/2$ *at* $\psi = 3\pi/2$ *or* $\psi = \pi/2$ *respectively. However since in these cases we have that:*

$$\frac{d^2}{d\psi^2}(h(x(\psi))) = 0, \tag{5.17}$$

the two sets meet at this point tangentially and do not cross over into the other hemisphere.

This concludes the proof. □

Remark 15. *In* [10] *it was observed that* ρ_{max} *of* $\mathbb{T}_+(p)$ *always corresponds to the trapped geodesic with* $x_{min}(\theta(p))$ *and* ρ_{min} *of* $\mathbb{T}_+(p)$ *always corresponds to the trapped geodesic with* $x_{max}(\theta(p))$ *. When* p *is outside the region of trapping* $h(x)|_{x_{max}}$ *is a local maximum of* $h(x(\psi))$ *(as a function of* ψ*) and* $h(x)|_{x_{min}}$ *is a local minimum of* $h(x(\psi))$*. When* p *is between the region of trapping and the horizon* $h(x)|_{x_{max}}$ *is a local minimum of* $h(x(\psi))$ *and* $h(x)|_{x_{min}}$ *is a local maximum of* $h(x(\psi))$*. Since outside* $\mathbb{T}_+(p)$ *is always described by* $\rho_2(\psi)$ *and inside by* $\rho_1(\psi)$*,* ρ_{min} *then always corresponds to* x_{min} *and* ρ_{max} *always corresponds to* x_{max}*. This also holds for* $p \in \mathcal{A}$*.*
This observation means that the null geodesic approaching the innermost photon orbit has the smallest impact parameter (deviation from the radially ingoing null geodesic) and the null geodesic approaching the outermost photon orbit has the largest impact parameter.
For $\mathbb{T}_-(p)$ *the correspondence is switched.*

Remark 16. *The parametrization for* $\sin(\psi)$ *breaks down on the rotation axis, the one for* $\sin(\rho)$ *however remains valid with only one possible value for* $x = r_3$*. Due to the symmetry at these points we know that* $\mathbb{T}_{\pm}(p)$ *are described by proper circles on the celestial sphere. The PND is aligned with the axis of the rotation symmetry and hence the sets are symmetric under rotation along* ψ*. The situation is therefore equivalent to Schwarzschild and an observer can not distinguish whether he observes a Schwarzschild black hole or a Kerr black hole in the direction of the rotation axis.*

Remark 17. *We have only proved Theorem 14 for one standard observer at any particular point. However since any other observer at this point is related to the standard observer by a Lorentz transformation and the Lorentz transformations act as conformal transformations on the celestial sphere* [16, p.14]*, the Theorem indeed holds for any observer. In* [9] *the quantitative effect on the shape of the shadow of boosts in different directions are discussed.*

Remark 18. *The parametrization for the trapped set on the celestial sphere of any standard observer in* [10, 11] *was derived for a much more general class of spacetimes. Therefore Theorem 14 might actually hold for these cases as well. However this is beyond the scope of this paper.*

From Theorem 14 we immediately get the following Corollary:

Corollary 19. *For any observer at any point* p *in the exterior region of a subextremal Kerr spacetime we have that for any* $k \in \mathbb{T}_+(p)$ *and any* $\epsilon > 0$

- $B_\epsilon(k) \cap \Omega_{\mathcal{H}^+}(p) \neq \emptyset$
- $B_\epsilon(k) \cap \Omega_{\mathcal{I}^+}(p) \neq \emptyset$.

So if we interpret the celestial sphere as initial data space for null geodesics starting at p, the Corollary is a coordinate independent formulation of the fact that trapping in the exterior region of subextremal Kerr black holes is unstable.
See Figure 5 as an example on how the trapped sets change under a variation of the radial location of the observer.

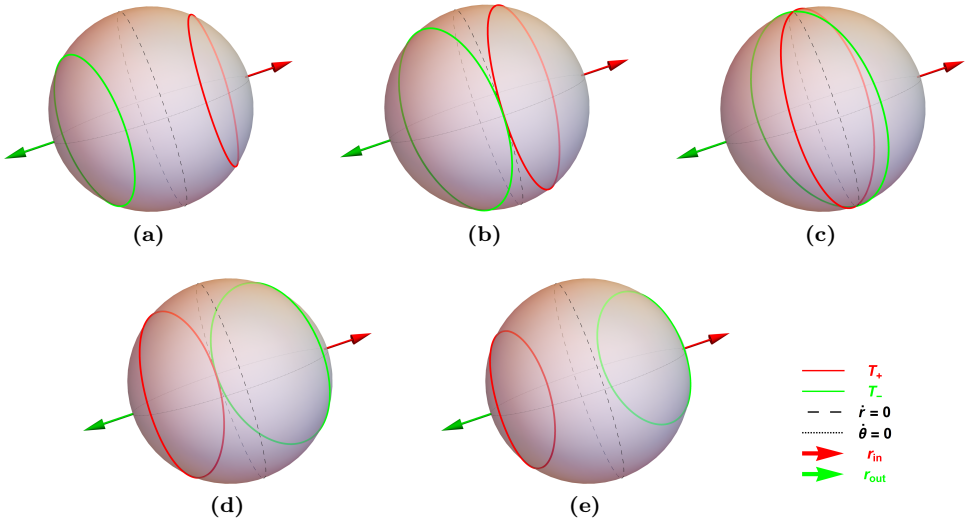

FIGURE 5. The trapped set on the celestial sphere of a standard observer at different radial locations in the equatorial plane of the exterior region of a Kerr black hole with $a = 0.9$. Observer (a) is located outside the region of trapping at $r = 5M$. Observer (b) is located on the outer boundary of the region of trapping at $r = r_2 = 3.535M$. Observer (c) is located inside the region of trapping at $r = r_3 = 2.56M$. Observer (d) is located on the inner boundary of the area of trapping at $r = r_1 = 1.73M$ Finally observer (e) is located between the horizon and the area of trapping at $r = 1.59M$. Again one can observe how the two trapped sets move in opposite directions on the celestial sphere as the observer approaches the black hole. In (a) the future trapped set is on the ingoing hemisphere and the past trapped set is on the outgoing hemispere. In (b) they meet in one point tangentially but are still entirely in one hemisphere except for that one point. In (a) the trapped sets intersect in two points and both have parts in both hemispheres. In (d) they only meet at one point tangentially again (now on the "other" side of the celestial sphere) and finally in (e) the future trapped set is entirely in the outgoing hemisphere and the past trapped set is entirely in the ingoing hemisphere.

Even though the qualitative features of $\mathbb{T}_\pm(p)$ do not change under a change of parameters, the quantitative features do. In [13, 14] it is discussed what information can be read of from the shadow at infinity. For points inside the manifold as considered in this work, it is unclear to the authors what the maximal amount of information is that an observer can obtain from the shape of the shadow. In the following we will present numerical calculations that suggest that the radial degeneracy of the shadow is broken in Kerr spacetimes away from the symmetry axis. We take the stereographic projection: [16, p.10]

$$\zeta = \frac{x + iy}{1 - z} \tag{5.18a}$$

$$x = \sin(\rho)\sin(\psi) \qquad y = \sin(\rho)\cos(\psi) \qquad z = \cos(\rho) \tag{5.18b}$$

of $\mathbb{T}_-(p)$ in order to compare the exact shape of the shadow for different observers. Here the values of ρ and ψ are given by the parametrization in (5.5). The above projection for the celestial sphere of a standard observer in the exterior region of

a Kerr black hole guarantees that projection of the shadow in the complex plane will have a reflection symmetry about the real axis. This is due to the symmetry of the shadow on the celestial sphere of a standard observer under a sign flip in the k_2 component. To compare conformal class of the shadow for observers in different points of different black hole spacetimes we establish the notion of a canonical observer together with a canonical projection. This will allow us to compare the shape of the shadow for these observers directly. The canonical observer together with the canonical projection are defined in such a way that the points on $\mathbb{T}_-(p)$ with $\Psi = \pi/2, 3\pi/2$ will correspond to the points $(1, 0)$ and $(-1, 0)$ in the complex plane. On the practical side we take the stereographic projection along the radially ingoing direction for the standard observer and then apply conformal transformations to the projection of the shadow (translation and rescaling). In the following C_{S^2} denotes the union of all conformal transformations on S^2.

Remark 20. *In order to prove that the conformal class of two curves x and y on S^2 are equal it is sufficient to find an $x_0 \in C_{S^2}[x]$ and a $y_0 \in C_{S^2}[y]$ such that $x_0 = y_0$. By choosing a canonical observer, we choose a fix representative $c_0[p] \in C_{S^2}[\mathbb{T}_-(p)]$ of each conformal class and thereby eliminate the freedom of performing conformal transformations on the celestial sphere of an observer. Hence if the shape of the canonical representative of any two shadows $c_0[p_1(a_1, \theta_1, r_1)]$, $c_0[p_2(a_2, \theta_2, r_2)]$ coincide, then their conformal class is equal. On the other hand if $c_0[p_1(a_1, \theta_1, r_1)] \neq c_0[p_2(a_2, \theta_2, r_2)]$ then the conformal classes of the shadow at p_1 and that at p_2 are different.*

Note that when investigating for degeneracies numerically only negative answers are reliable, because an apparent degeneracy could simply be due to the fact that the difference between the shadows of two canonical observers is below the scale of the numerical resolution. The apparent breaking of the radial degeneracy in Kerr spacetimes can be seen in Figure 6, where we plotted two black hole shadows, for canonical observers located in a Kerr spacetime with $a = 0.99$, at $\theta = \pi/2$, and different r values: $r_1 = 5, r_2 = 50$. These particular values were chosen because for this case the degeneracy breaking is visible by the naked eye from the plot in Figure 6. In general the breaking of the radial degeneracy is hardly visible in the plot. Establishing a rigorous proof for the breaking of the radial degeneracy, as well as investigation the possibility for the shadow to have some complicated degeneracy of the form $f(a, r, \theta) = const.$, where f is function of these parameters, is subject for further investigations. The breaking of the radial degeneracy implies that in principle when observing the shadow of a black hole, as intended by the Event Horizon Telescope, one would have to take the distance from said black hole into consideration when trying to extract the black holes parameters from the observation. However the influence of the radial degeneracy for far away observers is quite likely a lot smaller than the resolution that can be achieved from such observations.

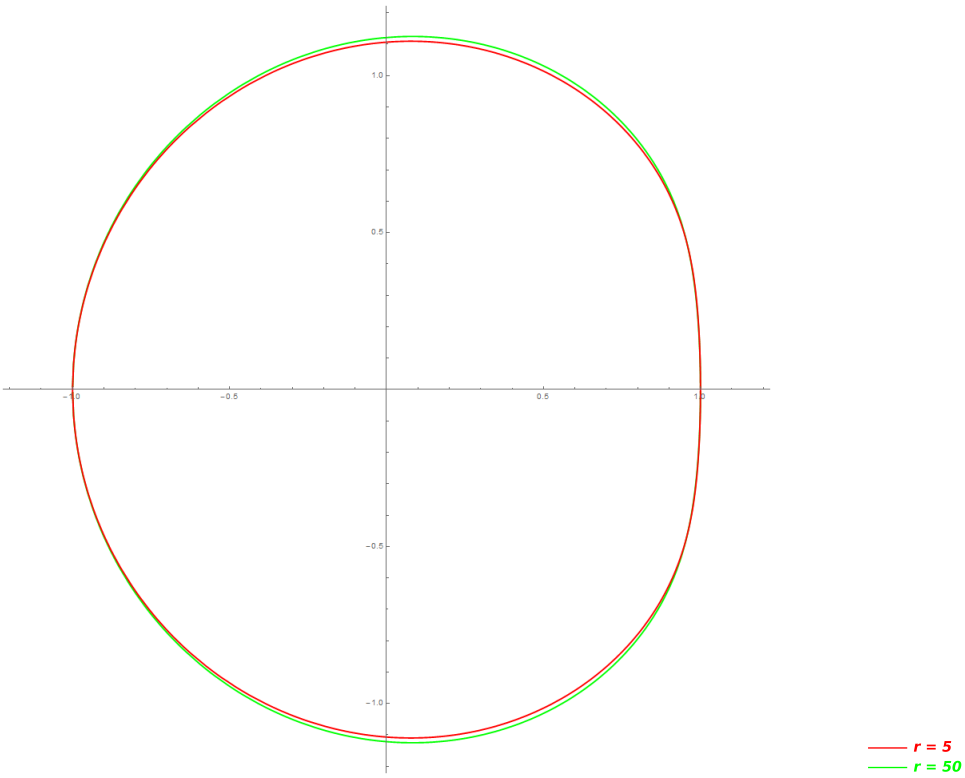

FIGURE 6. Breaking of the radial degeneracy for the shadow of a Kerr black hole. Two canonical observers with $a = 0.99$, at $\theta = \pi/2$, for two different values $r = 5$ and $r = 50$.

6. Application

Everything we have derived about the behaviour of null geodesics in Kerr spacetimes can be represented in a couple of simple plots. See Figure 7, Figure 4 and Figure 5 as examples; in the Mathematica notebook provided with this paper [1] the parameters a/M and $\mathcal{Q}$ as well as the location of the observer $\{r(p), \theta(p)\}$ can be varied. This allows one to develop an intuitive understanding of the influence of these parameters.

Furthermore by the eikonal approximation it is clear, that a massless wave equation should relate to the null geodesic equation in the limit of high frequencies. In [7] it is shown that when separating the wave equation $\Sigma\Box\psi = 0$ the ODE for the radial function in Schrödinger form can be written as:

$$\frac{\mathrm{d}^2 u}{\mathrm{d}r^{*\,2}} + \left(\frac{R(r, E = \omega, L_z = m, L^2 = \lambda_{lm})}{(r^2 + a^2)^2} - F(r) \right) u = 0 \tag{6.1}$$

with $F(r) = \frac{\Delta}{r^2+a^2}(a^2\Delta + 2Mr(r^2 - a^2)) \geq 0$ and hence we have the following relations:

$$\omega \sim E, \qquad m \sim L_z, \qquad \lambda_{lm} \sim L^2. \tag{6.2}$$

When trying to understand the different treatments of different parameter ranges in [7] it is helpful to play with the parameters of the pseudo potential in the Mathematica notebook provided with this paper [1]. The construction of the different mode currents becomes much more intuitive when thinking about where in Figure 7 the corresponding parameters are located. Note that in the high frequency limit the pseudo potentials correspond to the location of $\omega^2 - V(r, \omega, m, \Lambda) = 0$ and hence

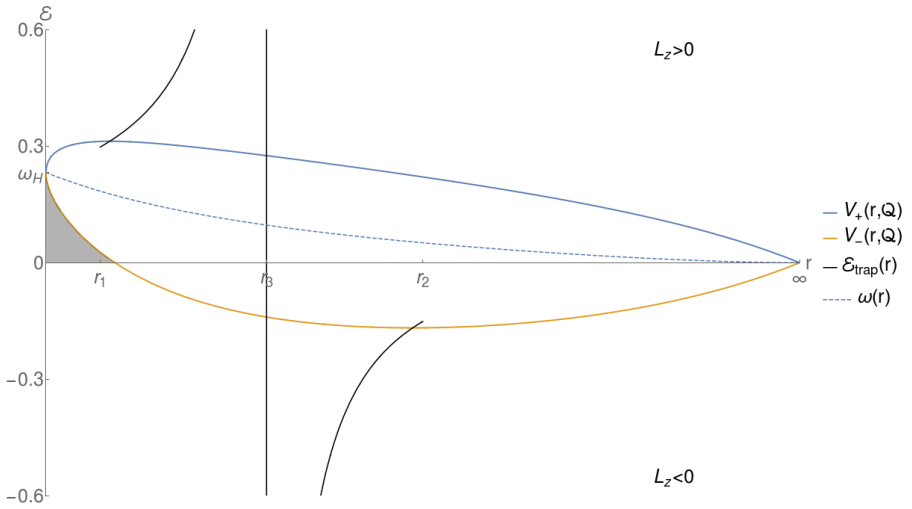

FIGURE 7. Plot of the pseudo potentials $V_\pm$ as function of a compactified radial coordinate in the exterior region for $a = 0.764$ and $\mathcal{Q} = 0.18$. Its qualitative features are preserved when a and $\mathcal{Q}$ are changed. The location of trapping in phase space is indicated by the function $\mathcal{E}_{trap}(r)$. The extrema of the pseudo potentials are the intersection of V_+ and V_- with this function. Therefore they slide on this curve as $\mathcal{Q}$ increases. The area filled in gray corresponds to geodesics with $E < 0$. It is clear from this plot that the regions occupied by geodesics of negative energy and trapped geodesics respectively are disjoint in phase space.

the location where the leading contribution to the bulk terms of the Q^y and Q^h currents change their sign.

Another interesting observation is that combining the results in section 4.2 and section 4.3 we can see that to separate trapping from the ergoregion in physical space it is sufficient if we restrict the null geodesics to be either co- or counter-rotating. In the co-rotating case there simply does not exist an ergoregion and the statement is clear. In the counter rotating case trapping is constrained to $r \in (r_3, r_2]$ and $r_3 > 2M \geq r_{ergo}$ for all Kerr spacetimes with $a < M$. In this direction particularly interesting might be the potential functions $\Psi_\pm$ in [12] which have interesting properties in physical space.

Acknowledgements. We are grateful to Lars Andersson, Volker Perlick and Siyuan Ma for helpful discussions and their comments on the manuscript.

APPENDIX A.

Let $f(x)$ be a smooth function on $[-1, 1]$ vanishing at the boundary points with a unique maximum with value 1 at zero. Hence $f(0) = 1$, $f'(0) = 0$ and $f''(0) < 0$. We then define:

$$g_{1a}(x) = \arcsin(f(x)) : \quad [-1, 0) \to [0, \pi/2) \tag{A.1}$$

$$g_{2a}(x) = \pi - \arcsin(f(x)) : \quad [-1, 0) \to (\pi/2, \pi] \tag{A.2}$$

$$g_{1b}(x) = \arcsin(f(x)) : \quad (0, 1] \to [0, \pi/2) \tag{A.3}$$

$$g_{2b}(x) = \pi - \arcsin(f(x)) : \quad (0, 1] \to (\pi/2, \pi] \tag{A.4}$$

Note that $g'_{1a/b}(x) = -g'_{2a/b}(x)$. We then calculate:

$$\frac{d}{dx} g_{1a}(x) = \frac{f'(x)}{\sqrt{1-f(x)^2}}. \tag{A.5}$$

Note that both the nominator and denominator vanish as x goes to zero. However to apply the rule of l'Hopital we have to consider the square of the expression. We then get:

$$\lim_{x\to 0} \left(\frac{d}{dx} \arcsin(f(x)) \right)^2 = \lim_{x\to 0} \frac{-f''(x)}{f(x)} = -f''(0). \tag{A.6}$$

Thus $d/dx(\arcsin(f(x)))|_{x=0} = \sqrt{-f''(0)}$. The sign is chosen based on the fact that $d/dx(\arcsin(f(x))) > 0$ for $x \in [1, 0)$. Note that on $[-1, 0)$ the derivative of $g_1(x)$ is positive while on $(0, 1]$ it is negative. Together this gives us that the function:

$$g(x) = \begin{cases} g_{1a}(x) & \text{if } x \in [-1, 0) \\ \pi/2 & \text{if } x = 0 \\ g_{2b}(x) & \text{if } x \in (0, 1] \end{cases} \tag{A.7}$$

is smooth at $x = 0$ and therefore on $[-1, 1]$ with $d/dx(g(x))|_{x=0} = \sqrt{-f''(0)}$.

References

1. *http://www.aei.mpg.de/KerrNullgeodesicsPlots*, (Direct URL to download of notebook).
2. J.M. Bardeen, *Black Holes 215-39*, CRC Press, January 1973 (en).
3. Brandon Carter, *Global Structure of the Kerr Family of Gravitational Fields*, Physical Review **174** (1968), no. 5, 1559–1571.
4. S. Chandrasekhar, *The mathematical theory of black holes*, Oxford Classic Texts in the Physical Sciences, The Clarendon Press, Oxford University Press, New York, 1998, Reprint of the 1992 edition. MR 1647491
5. P. M. Cohn, *Algebra. Volume 1. Second Edition*, 2nd edition ed., Wiley, Chichester Sussex ; New York, July 1982 (English).
6. Pedro V. P. Cunha, Carlos A. R. Herdeiro, Eugen Radu, and Helgi F. Runarsson, *Shadows of Kerr black holes with and without scalar hair*, International Journal of Modern Physics D **25** (2016), no. 09, 1641021, arXiv: 1605.08293.
7. M. Dafermos, I. Rodnianski, and Y. Shlapentokh-Rothman, *Decay for solutions of the wave equation on Kerr exterior spacetimes III: The full subextremal case $|a| < M$*, (2014), arXiv.org:1402.7034.
8. Sheperd S. Doeleman, Jonathan Weintroub, Alan E. E. Rogers, Richard Plambeck, Robert Freund, Remo P. J. Tilanus, Per Friberg, Lucy M. Ziurys, James M. Moran, Brian Corey, Ken H. Young, Daniel L. Smythe, Michael Titus, Daniel P. Marrone, Roger J. Cappallo, Douglas C.-J. Bock, Geoffrey C. Bower, Richard Chamberlin, Gary R. Davis, Thomas P. Krichbaum, James Lamb, Holly Maness, Arthur E. Niell, Alan Roy, Peter Strittmatter, Daniel Werthimer, Alan R. Whitney, and David Woody, *Event-horizon-scale structure in the supermassive black hole candidate at the Galactic Centre*, Nature **455** (2008), 78–80.
9. Arne Grenzebach, *Aberrational Effects for Shadows of Black Holes*, arXiv:1502.02861 [gr-qc] (2015), arXiv: 1502.02861.
10. Arne Grenzebach, Volker Perlick, and Claus Lämmerzahl, *Photon regions and shadows of Kerr-Newman-NUT black holes with a cosmological constant*, Physical Review D **89** (2014), no. 12, 124004.
11. Arne Grenzebach, Volker Perlick, and Claus Lämmerzahl, *Photon Regions and Shadows of Accelerated Black Holes*, International Journal of Modern Physics D **24** (2015), no. 09, 1542024, arXiv: 1503.03036.
12. Wolfgang Hasse and Volker Perlick, *A Morse-theoretical analysis of gravitational lensing by a Kerr-Newman black hole*, Journal of Mathematical Physics **47** (2006), no. 4, 042503, arXiv: gr-qc/0511135.
13. Kenta Hioki and Kei-ichi Maeda, *Measurement of the Kerr spin parameter by observation of a compact object's shadow*, Physical Review D **80** (2009), no. 2, 024042.
14. Zilong Li and Cosimo Bambi, *Measuring the Kerr spin parameter of regular black holes from their shadow*, Journal of Cosmology and Astroparticle Physics **2014** (2014), no. 01, 041–041, arXiv: 1309.1606.
15. Barrett O'Neill, *The Geometry of Kerr Black Holes*, reprint edition ed., Dover Publications, January 2014 (Englisch).

16. Roger Penrose and Wolfgang Rindler, *Spinors and Space-Time: Volume 1, Two-Spinor Calculus and Relativistic Fields*, Cambridge University Press, Cambridge u.a., May 1987 (English).
17. Gabriela Slezakova, *Geodesic Geometry of Black Holes*, Thesis, The University of Waikato, 2006.
18. J. L. Synge, *The escape of photons from gravitationally intense stars*, Monthly Notices of the Royal Astronomical Society **131** (1966), 463.
19. Edward Teo, *Spherical Photon Orbits Around a Kerr Black Hole*, General Relativity and Gravitation **35** (2003), no. 11, 1909–1926 (en).
20. Daniel C. Wilkins, *Bound geodesics in the kerr metric*, Physical Review D **5** (1972), no. 4, 814–822.